REPORT DOCUMENTATION PAGE

Form Approved OMB NO. 0704-0188

1. REPORT DATE (DD-MM-YYYY)	2. REPORT TYPE	3. DATES COVERED (From - To)
08-12-2021	Final Report	1-May-2020 - 30-Apr-2021

4. TITLE AND SUBTITLE
Final Report: Numerical Parallel Scalability of the Shifted Boundary Method

5a. CONTRACT NUMBER
W911NF-20-1-0045

5b. GRANT NUMBER

5c. PROGRAM ELEMENT NUMBER
611103

6. AUTHORS

5d. PROJECT NUMBER

5e. TASK NUMBER

5f. WORK UNIT NUMBER

7. PERFORMING ORGANIZATION NAMES AND ADDRESSES
Duke University
C/O Office of Research Support
2200 W. Main St., Ste. 710
Durham, NC 27705 -4677

8. PERFORMING ORGANIZATION REPORT NUMBER

9. SPONSORING/MONITORING AGENCY NAME(S) AND ADDRESS (ES)
U.S. Army Research Office
P.O. Box 12211
Research Triangle Park, NC 27709-2211

10. SPONSOR/MONITOR'S ACRONYM(S)
ARO

11. SPONSOR/MONITOR'S REPORT NUMBER(S)
75805-MA-RIP.3

12. DISTRIBUTION AVAILIBILITY STATEMENT
Approved for public release; distribution is unlimited.

13. SUPPLEMENTARY NOTES
The views, opinions and/or findings contained in this report are those of the author(s) and should not contrued as an official Department of the Army position, policy or decision, unless so designated by other documentation.

14. ABSTRACT

15. SUBJECT TERMS

16. SECURITY CLASSIFICATION OF:			17. LIMITATION OF ABSTRACT	15. NUMBER OF PAGES	19a. NAME OF RESPONSIBLE PERSON
a. REPORT	b. ABSTRACT	c. THIS PAGE			Guglielmo Scovazzi
UU	UU	UU	UU		19b. TELEPHONE NUMBER 919-660-5075

RPPR Final Report
as of 09-Dec-2021

Agency Code: 21XD

Proposal Number: 75805MARIP **Agreement Number: W911NF-20-1-0045**
INVESTIGATOR(S):

Name: Guglielmo Scovazzi
Email: guglielmo.scovazzi@duke.edu
Phone Number: 9196605075
Principal: Y

Organization: **Duke University**
Address: C/O Office of Research Support, Durham, NC 277054677
Country: USA

DUNS Number: 044387793 EIN: 560532129
Report Date: 31-Jul-2021 Date Received: 08-Dec-2021
Final Report for Period Beginning 01-May-2020 and Ending 30-Apr-2021
Title: Numerical Parallel Scalability of the Shifted Boundary Method
Begin Performance Period: 01-May-2020 **End Performance Period:** 30-Apr-2021
Report Term: 0-Other

Submitted By: Guglielmo Scovazzi Email: guglielmo.scovazzi@duke.edu
Phone: (919) 660-5075

Distribution Statement: 1-Approved for public release; distribution is unlimited.

STEM Degrees: 1 **STEM Participants:**

Major Goals: The PI was sponsored by the Mathematical Sciences Division of the Army Research Office (ARO) through Grant W911NF1810308 titled ``The shifted interface method for solid mechanics: An embedded domain approach.'' In this sponsored research, the PI and his team at Duke University are developing embedded (or immersed) finite element numerical methods for solid mechanics applications, as a paradigm of computational mechanics applications.

Specifically, through the ARO Grant W911NF1810308, the PI and his research group have developed a new embedded finite element method, named ``Shifted Boundary Method'' (or SBM). This new approach overcomes the difficulty on matrix conditioning and algorithmic stability that the occurrence of small cut cells produced in standard embedded methods. This without creating complicated data structures and limiting - in general - computational complexity to a minimum. The key feature of the SBM is the idea of shifting the location where boundary conditions are applied from the true to the surrogate boundary, and to appropriately modify the shifted boundary conditions, enforced weakly, in order to preserve optimal convergence rates of the numerical solution. This process yields a method that is simple, robust, and efficient.

One aspect not covered by the ARO Grant W911NF1810308 is the analysis of performance of the SBM in the context of parallel computing architectures. It was expected from previous experience that the SBM would show good overall parallel scalability. Certainly the setup phase is naturally parallel in nature, since it requires the computation of the three-dimensional intersections and distances between the computational grid and the geometric shapes to be simulated. However a few open questions remained on the preconditioning of the algebraic system of equations associated with the SBM in large-scale computations.

This ARO Grant W911NF2010045 allowed the PI to purchase a high-performance computing cluster and test the hypotheses mentioned above. The PI studied the scalability of the SBM in an engineering application that could be relevant to the mission and vision of ARO in the realm of additive manufacturing and similar or related applications. The computational outcomes have shown that the SBM maintains good scalability up to the largest problems attempted, on the order of 20 million elements. Problems of this size are about the largest computational grids that fit on the purchased computing cluster, and the typical size for applied engineering applications.

Accomplishments: The cluster was successfully installed and deployed. We tested the proposed algorithms as planned and their scalability was shown on computational grids up to about 20-25 million elements.

The results showed that the parallel scalability of the proposed method is identical to a standard finite element

method based on linear interpolation of the displacement field (the standard in finite elements).

This is a very encouraging outcome for the future of the shifted boundary method, in the sense that the PI was able to prove that for typical industrial size simulation the cost and scalability of the shifted boundary method is the same as traditional finite elements based on body-fitted grids.

The preprocessing phase of the shifted boundary method was already tested and demonstrated to be fully scalable in previous work. The funded work concludes an important evaluation of the shifted boundary method for applied engineering problems.

Training Opportunities: During the process of deployment and installation of the requested high-performance computing cluster, two Ph.D. students were trained to optimize the algorithms for optimal scalability.

The purchase of the cluster had the positive outcome of also helping graduate research assistants to develop advanced computing and software development skills.

Results Dissemination: Some of the results of the scalability tests performed were published in archive journal articles.

Honors and Awards: The PI was named distinguished lecturer at POSTECH (Pohang University of Science and Technology, South Korea)

Protocol Activity Status:

Technology Transfer: Nothing to Report

PARTICIPANTS:

Participant Type: PD/PI
Participant: Guglielmo Scovazzi
Person Months Worked: 1.00 **Funding Support:**
Project Contribution:
National Academy Member: N

Participant Type: Graduate Student (research assistant)
Participant: Kangan Li
Person Months Worked: 12.00 **Funding Support:**
Project Contribution:
National Academy Member: N

Participant Type: Postdoctoral (scholar, fellow or other postdoctoral position)
Participant: Nabil Atallah
Person Months Worked: 12.00 **Funding Support:**
Project Contribution:
National Academy Member: N

ARTICLES:

RPPR Final Report
as of 09-Dec-2021

Publication Type: Journal Article Peer Reviewed: Y **Publication Status:** 1-Published
Journal: International Journal for Numerical Methods in Engineering
Publication Identifier Type: DOI Publication Identifier: 10.1002/nme.6779
Volume: 122 Issue: 20 First Page #: 5935
Date Submitted: 12/7/21 12:00AM Date Published: 7/1/21 4:00AM
Publication Location:
Article Title: The shifted boundary method for solid mechanics
Authors: Nabil M. Atallah, Claudio Canuto, Guglielmo Scovazzi
Keywords: approximate boundary conditions, complex geometry, imaging-to-computing, shifted boundary method, solid mechanics, unfitted finite elements
Abstract: We propose a new embedded/immersed framework for computational solid mechanics, aimed at vastly speeding up the cycle of design and analysis in complex geometry. In many problems of interest, our approach bypasses the complexities associated with the generation of CAD representations and sub- sequent body-fitted meshing, since it only requires relatively simple repre- sentations of the surface geometries to be simulated, such as collections of disconnected triangles in three dimensions, widely used in computer graph- ics. Our approach avoids the complex treatment of cut elements, by resorting to an approximate boundary representation and a special (shifted) treatment of the boundary conditions to maintain optimal accuracy. Natural applications of the proposed approach are problems in biomechanics and geomechanics, in which the geometry to be simulated is obtained from imaging techniques. Sim- ilarly, our computational framework can easily treat geometries that are the result of ...
Distribution Statement: 2-Distribution Limited to U.S. Government agencies only; report contains proprietary info
Acknowledged Federal Support: **Y**

Publication Type: Journal Article Peer Reviewed: Y **Publication Status:** 1-Published
Journal: International Journal for Numerical Methods in Engineering
Publication Identifier Type: DOI Publication Identifier: 10.1002/nme.6806
Volume: 122 Issue: 22 First Page #: 6641
Date Submitted: 12/7/21 12:00AM Date Published: 9/1/21 4:00AM
Publication Location:
Article Title: The shifted fracture method
Authors: Kangan Li, Nabil M. Atallah, Antonio Rodríguez?Ferran, Dakshina M. Valiveti, Guglielmo Scovazzi
Keywords: approximate boundary conditions, embedded methods, extended finite element method, fracture mechanics, shifted boundary method, shifted interface method
Abstract: We propose a new framework for fracture mechanics, based on the idea of an approximate fracture geometry representation combined with approximate interface conditions. Our approach evolves from the shifted interface method, and introduces the concept of an approximate fracture surface composed of the full edges/faces of an underlying grid that are geometrically close to the true fracture geometry. The original interface conditions are then modified on the surrogate fracture geometry, by way of Taylor expansions. The shifted fracture method does not require cut cell computations or complex data structures, since the behavior of the true fracture is mimicked with standard integrals on the approximate fracture surface. Furthermore, the energetics of the true fracture are represented within the accuracy of the underlying polynomial finite ele- ment approximation and independently of the grid topology. The computational framework is presented here in its generality and then applied in ...
Distribution Statement: 2-Distribution Limited to U.S. Government agencies only; report contains proprietary info
Acknowledged Federal Support: **Y**

RPPR Final Report
as of 09-Dec-2021

Partners

,

I certify that the information in the report is complete and accurate:
Signature: Guglielmo Scovazzi
Signature Date: 12/8/21 8:58PM

Final Report: Award W911NF2010045
Numerical Parallel Scalability of the Shifted Boundary Method

Summary

Thanks to the support if ARO Award W911NF-18-1-0308, the PI's research team at Duke University developed a new embedded/immersed framework for computational solid mechanics, aimed at vastly speeding up the cycle of design and analysis in complex geometry. See the final report on that project for more details

Thanks to this DURIP award, the PI's research team was able to perform large scale three-dimensional computations and in particular to show that the Shifted Boundary Method (SBM) is as fast as a body-fitted displacement based finite element, on computational grids up to and above 20 million element in size. This is a very important result, since the setup phase of the SBM (comprising geometry acquisition, mesh generation, geometric immersion and definition of boundary conditions data structures) is only seconds or minutes, compared to hours, days or months in the case of body-fitted meshing.

1. Performance Assessment: Accuracy vs. computing time

To start, we present an accuracy test three dimensions, in which the efficiency of the SBM is compared against a standard, body-fitted, FEM, relying on a primal displacement formulation with piecewise-linear interpolation spaces and strong boundary conditions. We compare only the time required to assemble and solve the algebraic systems of equations, and point the reader to Section 2 for a comparative analysis of the simulation setup time, required to acquire the geometrical information and build the appropriate data structures.

1.1. Three-dimensional SBM performance test: A rectangular cuboid with holes

We consider here a three-dimensional non-convex domain with a boundary that includes smooth surfaces as well as sharp corners. As shown in Figure 1a, the linear isotropic elastostatics equations are computed in the domain $\Omega = \Omega_1 \setminus (\Omega_2 \cup \Omega_3)$, where Ω_1 is a rectangular cuboid centered at $[0, 0, 0]$ of length $L = 5$, width $W = 3.5$ and height $H = 3.5$, Ω_2 is a cube of side of length $S = 1.5$ and centered at $[-1.25, 0, 0]$ and Ω_3 is a sphere centered at $[1.25, 0, 0]$ with diameter $D = 1.5$. Consequently, we set $\bar{l}(\Omega) = 5$ which is the longest dimension of the bounding box of Ω. We consider the following manufactured solution

$$\boldsymbol{u} = \left\{ \begin{array}{c} u_x \\ u_y \\ u_z \end{array} \right\} = \frac{1}{10} \left\{ \begin{array}{c} -\cos(\pi x)\sin(\pi y)\cos(\pi z) \\ \sin(\pi x/7)\sin(\pi y/3)\cos(\pi z/5) \\ \sin(\pi xyz/2) \end{array} \right\}, \tag{1}$$

with a Young's modulus $E = 200 \cdot 10^6$ MPa and a Poisson's ratio $\nu = 0.3$. We apply the method of manufactured solutions. Figure 1b depicts, on a coarse grid, the surrogate domain, the surrogate

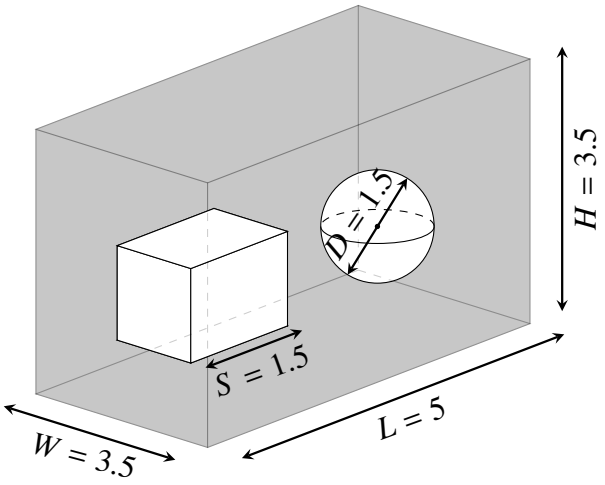

(a) Geometric setup of the problem (domain Ω and dimensions).

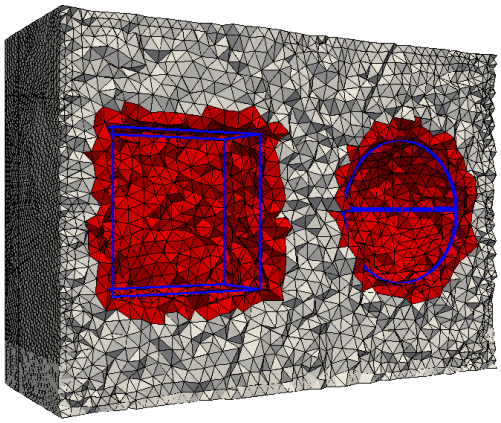

(b) Display of the surrogate domain $\tilde{\Omega}_h$ (grey and red), the true boundary Γ, and the layer $\tilde{\Omega}_h^\ell$ (red) for the SBM.

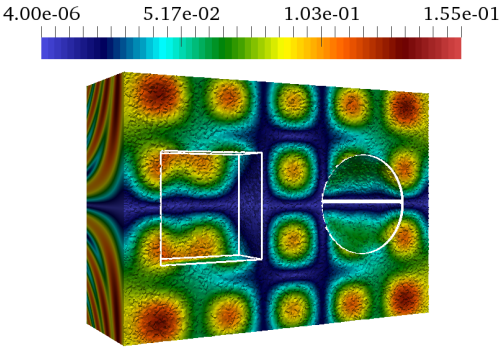

(c) Displacement magnitude.

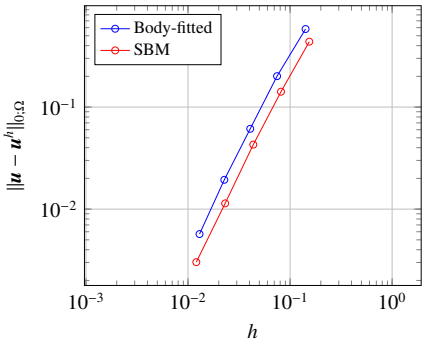

(d) L^2-error convergence for the SBM formulation and a body-fitted primal formulation.

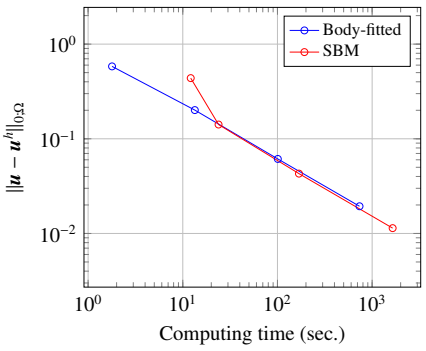

(e) L^2-error vs. computing time for the SBM formulation and a body-fitted primal formulation.

Figure 1: Three-dimensional test: Problem setup, displacement magnitude, convergence rates and computing times for the SBM formulation. Results with a primal body-fitted FEM with strong boundary conditions are plotted for reference.

boundary, and the layer of elements $\tilde{\Omega}_h^\ell$ attached to the surrogate boundary, used in the SBM formulation.

In this test, the boundary $\partial\Omega_2 \cup \partial\Omega_3$ are immersed while $\partial\Omega_1$ is body-fitted. Dirichlet boundary conditions are strongly enforced on $\partial\Omega_1$, while Neumann boundary conditions are enforced on $\partial\Omega_2 \cup \partial\Omega_3$ using the SBM approach. Also in this case, computations are performed on a single computing core, since both the SBM and the body-fitted FEM utilize the same procedures for parallelization, and a comparative study of parallel scalability is beyond the scope of this project.

Figure 1d shows that optimal L_2-convergence rates for the displacement is obtained using the SBM formulation, despite the theoretical estimate of $3/2$ in [3]. Note that, the SBM L_2-displacement error is lower than its body-fitted counterpart. This can be attributed to the slightly poorer mesh quality of the body-fitted meshes that are automatically generated to fit the boundaries. With respect to the corresponding SBM background grids, the body-fitted meshes have at least 1.5 times more elements with a ratio of the circumscribed/inscribed sphere diameters larger than two. This also seem to affect the overall computing time of the primal body-fitted FEM, as observed in Figure 1e: The SBM and body-fitted FEM have virtually the same rate and constant in the plot of the error versus computing time. This indicates that, for a desired level of accuracy, the SBM and the body-fitted FEM require the same computing time.

This test, despite its simplicity, is very important for understanding the performance of the SBM formulation with respect to a standard FEM formulation in practical applications. In a body-fitted grid, some nodes must lie on the boundaries, and this constraint inevitably has an effect on the mesh quality, and ultimately the overall computational efficiency of the algebraic solve. This trend is more pronounced for grids of larger size, often required in practical large-scale simulations.

2. Three-dimensional, complex-geometry, large-scale simulations

We consider next three tests with geometries that are progressively challenging for existing body-fitted mesh generation tools, and are representative of typical computational scenarios in the study of solid micro-structure, in biomedical design, and in geomechanics.

Table (1) shows the setup times for each of the three-dimensional tests. The SBM setup time includes the time it takes to: a) compute intersections between the STL surface that defines the boundary and the background grid; b) generate the surrogate domain and boundaries; and c) calculate the distance vector $\boldsymbol{d}$ along the surrogate boundary. To have a reference, the SBM setup time must be compared with the time it takes, in a body-fitted computation, to convert STL to CAD format, including geometry cleanup operations, and the time it takes to mesh the geometry.

Geometry	No. elements	No. active elements	No. cores	No. true surface facets	setup time (s)
Sponge (Section (2.1))	11,498,942	5,758,480	288	138,078	77
Stent (Section (2.2))	66,023,424	10,303,826	600	46,484	91
Porous rock (Sec. (2.3))	5,229,000	3,458,639	240	112,629	217

Table 1: Setup times for the three-dimensional tests.

Observe that the setup time for the porous rock problem is higher - in a relative sense - than the other problems. This is due to the fact that the rock surface is obtained from segmenting a CT-scan image, which contains several geometric artifacts. In particular, some disconnected pockets

are present on the rock surface and need to be removed in a preprocessing phase. We point out that this initial geometry cleanup phase is completely automated and parallelized, as opposed to the typical geometry cleanup in body-fitted grids and/or CAD models, which requires the direct intervention of the user.

In any case, since all setup times fall below 4 minutes, it is fair to state that the setup phase for the SBM is smaller, by one to two orders of magnitude, than the typical, current setup times required by CAD and body-fitted grid generation tools.

For all tests described below, the material is isotropic elastic with bulk and shear moduli equal to 1 GPa and 100 MPa, respectively. The corresponding Poisson ratio is $14/31 (\approx 0.452)$.

All computational results were obtained using the SBM formulation. Note also that the stresses shown in the figures are obtained from the displacement gradients as piecewise constant elemental quantities.

2.1. Sponge-like solid

In this section, we consider a domain with a sponge-like geometry [4], shown at the top left of Figure 2, as a representative of microstructures in porous media, weaved materials, and the like. The computational domain is the box $\Omega = [-10, -10] \times [-10, -10] \times [-10, 6]$ mm^3 with the surrogate boundary is shown at the top right of Figure 2.

The displacement on the left side surface is set to $\boldsymbol{u}^T = \{-0.04 \ , \ 0.0 \ , \ 0.0\}$ mm, while the solid is clamped ($\boldsymbol{u} = \boldsymbol{0}$) at the opposite surface (not seen). Traction-free boundary conditions are imposed elsewhere.

Numerical results, in terms of the magnitude of displacements, the volumetric stress, and von Mises stresses are shown in the three bottom rows of Figure 2. The smoothness of the computed fields indicates that the SBM can robustly address solid mechanics applications across very complex geometries and in scenarios beyond the hypotheses of applicability of the theoretical analysis of the SBM.

2.2. Stent specimen

As a prototypical geometry from biomedical applications, we consider here the stent [1] shown in Figure 3. The computational domain is immersed in a hollow cylindrical mesh with the surrogate boundary shown at the top right of Figure 3.

The displacement on the right end surface (not seen in Figure 3) is set to

$$\boldsymbol{u} = \{2.5y \text{ mm} \, , \ -2.5x \text{ mm} \, , \ -0.5\text{mm} \}^T \, ,$$

while the solid is clamped ($\boldsymbol{u} = \boldsymbol{0}$) at the opposite surface. Traction-free boundary conditions are imposed elsewhere.

Numerical results, in terms of the magnitude of displacements, the volumetric stress, and von Mises stresses are shown in the three bottom rows of Figure 3, and are again characterized by a smooth behavior.

2.3. Porous rock

Finally, we consider a domain with a geometry that has been obtained via imaging techniques [2]. As shown at the top left of Figure 4, we consider a sample of a porous rock, that is the domain $\Omega = [0, 0.3]$ mm $\times [0, 0.5]$ mm $\times [0.2, 0.47]$ mm, that has been subdivided in voxels

of size $8.33 \cdot 10^{-03}$ mm $\times$ $8.33 \cdot 10^{-03}$ mm $\times$ $8.33 \cdot 10^{-03}$ mm, by CT-scan techniques. The voxel representation of the sample has then been segmented, to represent the interface between the rocks and the voids in STL format (i.e., a set of disconnected triangular facets, which do not necessarily combine to form a water-tight surface).

The displacement on the top side surface is set to $\boldsymbol{u} = \{0.0\text{mm}\,,\, -5.4 \cdot 10^{-04}\text{mm}\,,\, 0.0\text{mm}\,\}^T$, while the solid is clamped ($\boldsymbol{u} = \boldsymbol{0}$) at the bottom surface. Traction-free boundary conditions are imposed elsewhere.

As apparent, the geometric features of this problem include a large number of fissures, holes and cracks which make body-fitted meshing very challenging, particularly since the (computational) interface rock/void is not water tight. It is in this situations that the power of an immersed/embedded solid mechanics method becomes clear, since the intersection of the interface solid/void with the background grid is an operation that is inherently parallelizable and much more robust and efficient than body-fitted mesh generation.

Numerical results are computed using the SBM formulation over the surrogate domain shown at the top right of Figure 4. The three bottom rows of Figures 4 display the displacement magnitude, volumetric stress, and von Mises stress, respectively. Much like in the previous three-dimensional tests, the numerical solution is smooth and well-behaved, indicating that the SBM can serve as a valuable tool in the emerging imaging-to-computing field.

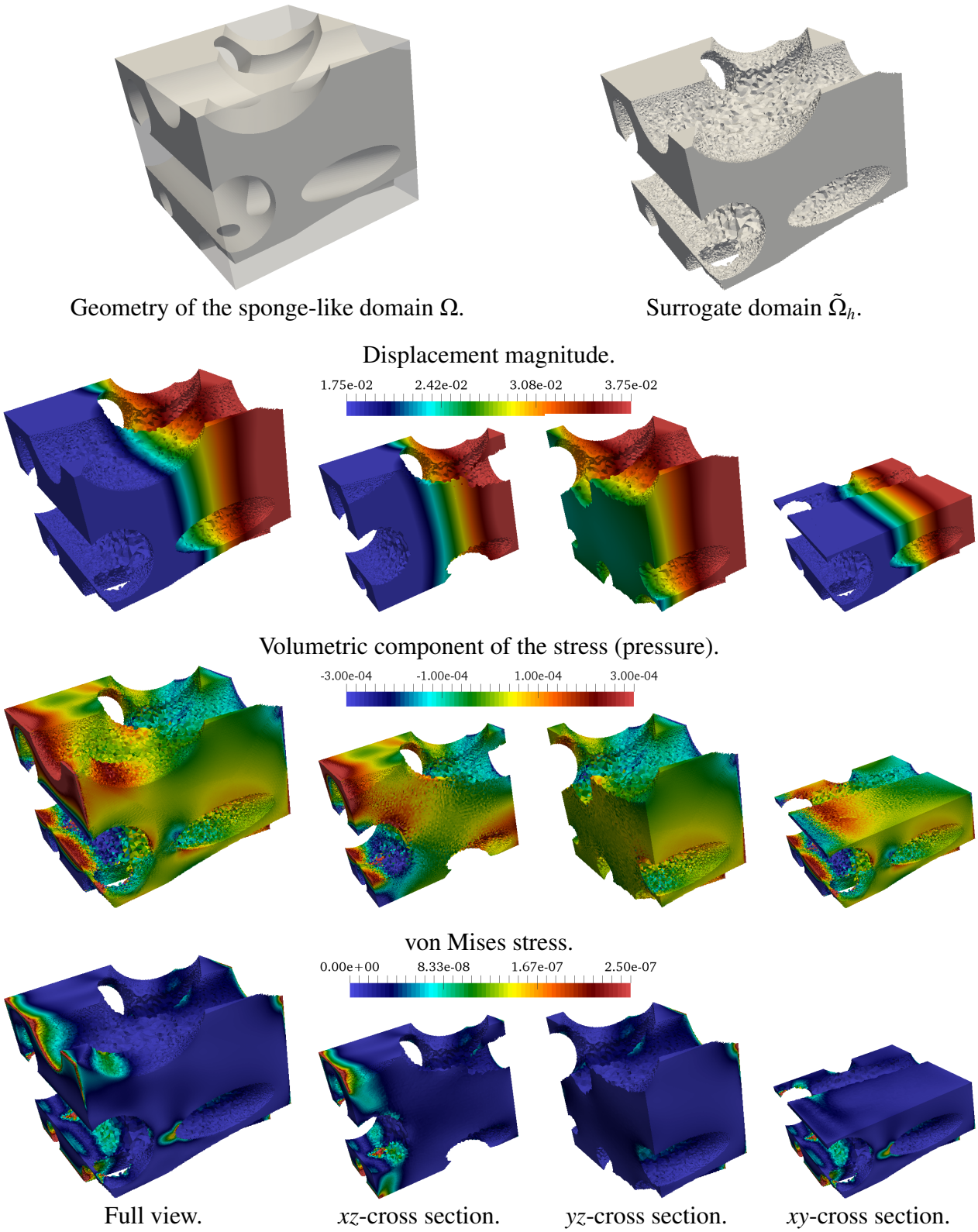

Figure 2: Sponge-like domain test. The geometry of the true domain Ω, the surrogate domain $\tilde{\Omega}_h$, and contours of the displacement magnitude, the volumetric (pressure) stress and the von Mises stress, for various cross-sections (mid-planes).

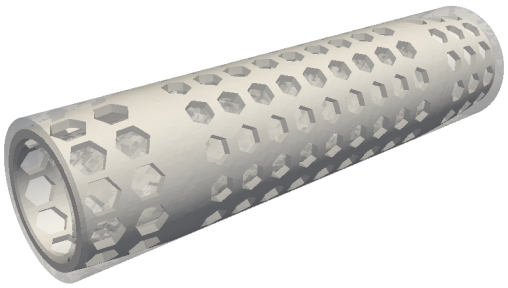

Geometry of the domain Ω.

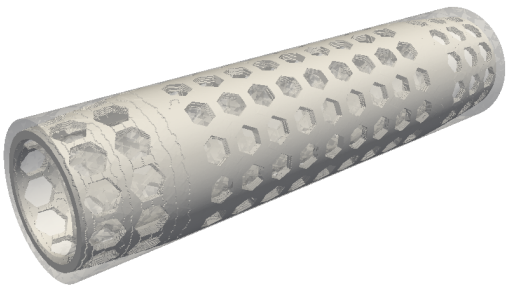

Surrogate domain $\tilde{\Omega}_h$.

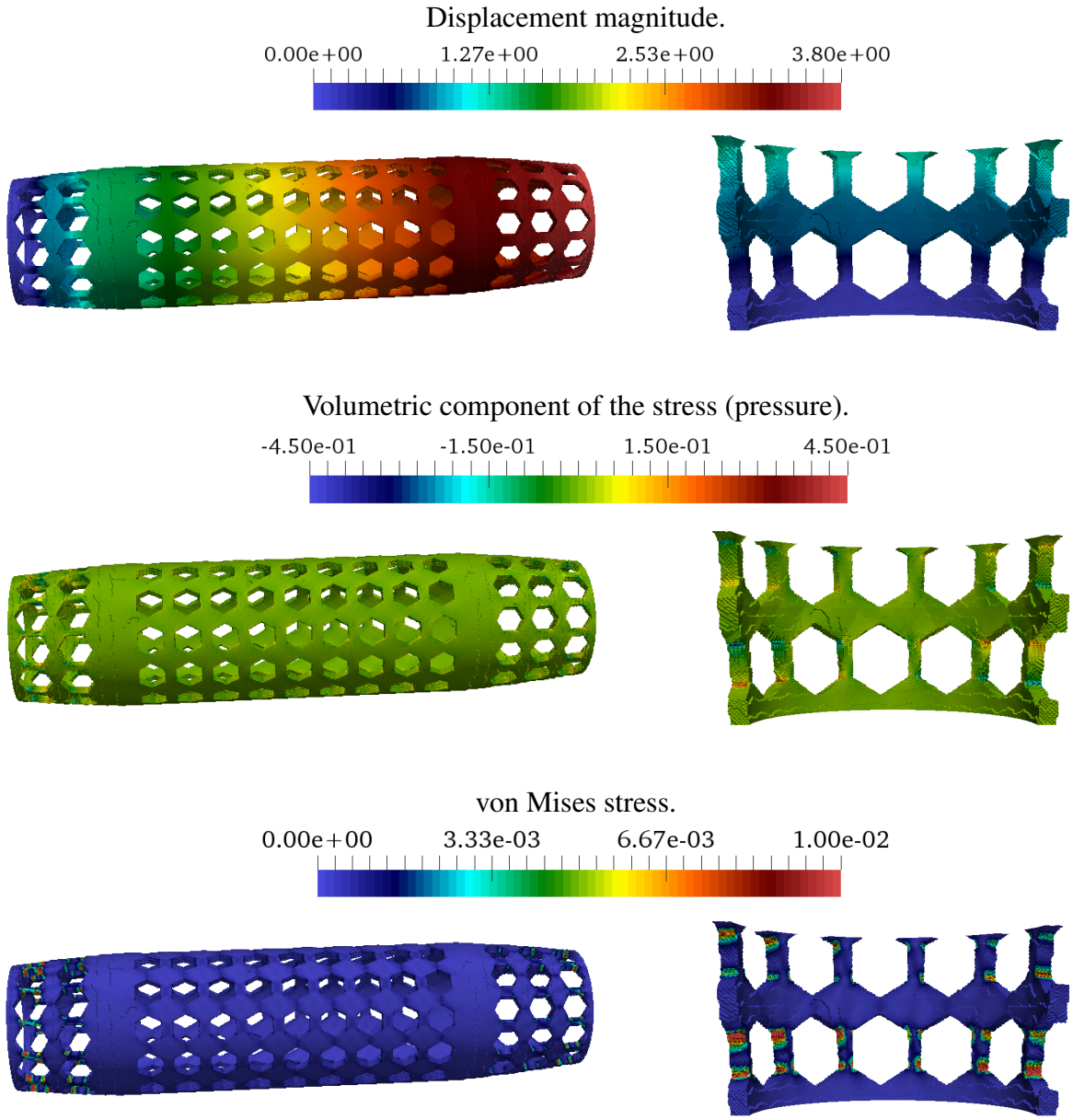

Figure 3: Stent domain test. The geometry of the true domain Ω, the surrogate domain $\tilde{\Omega}_h$, and contours of the displacement magnitude, the volumetric (pressure) stress and the von Mises stress, and a close-up view on high-stress regions.

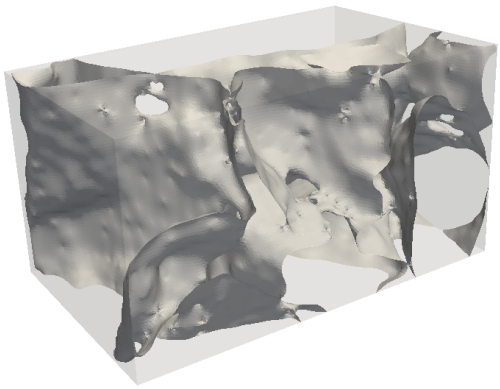

Geometry of the porous rock domain Ω.

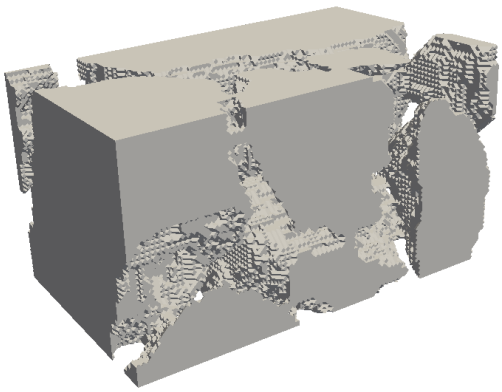

Surrogate domain $\tilde{\Omega}_h$.

Displacement magnitude.

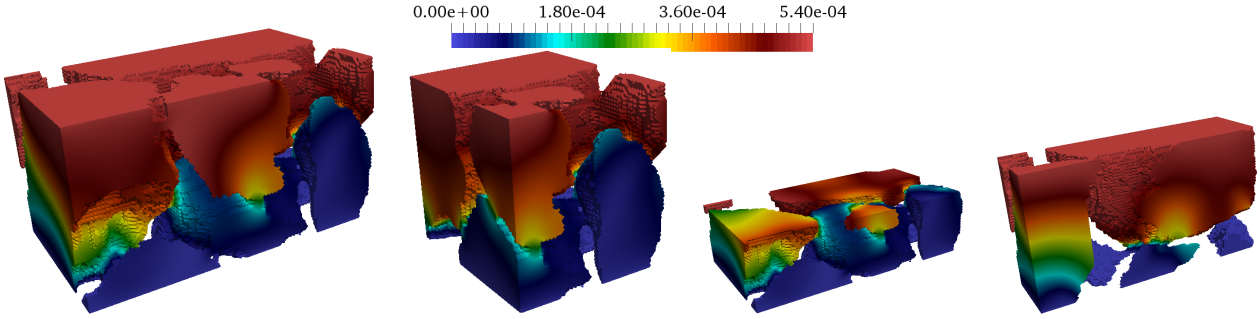

Volumetric component of the stress (pressure).

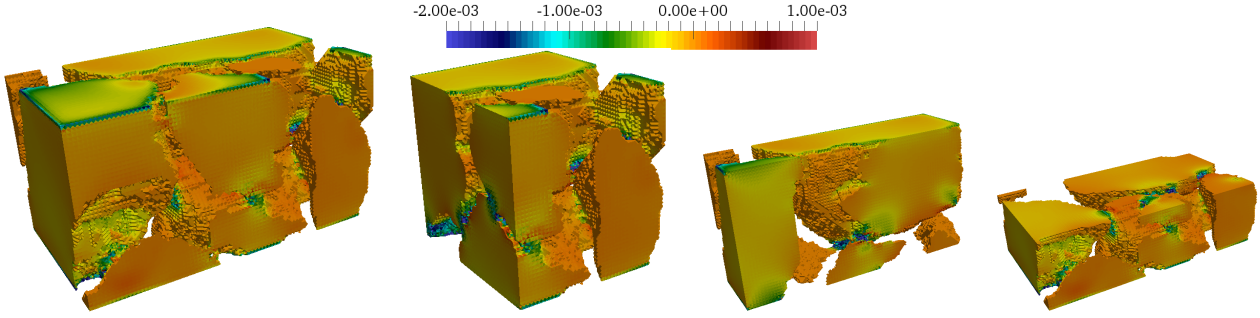

von Mises stress.

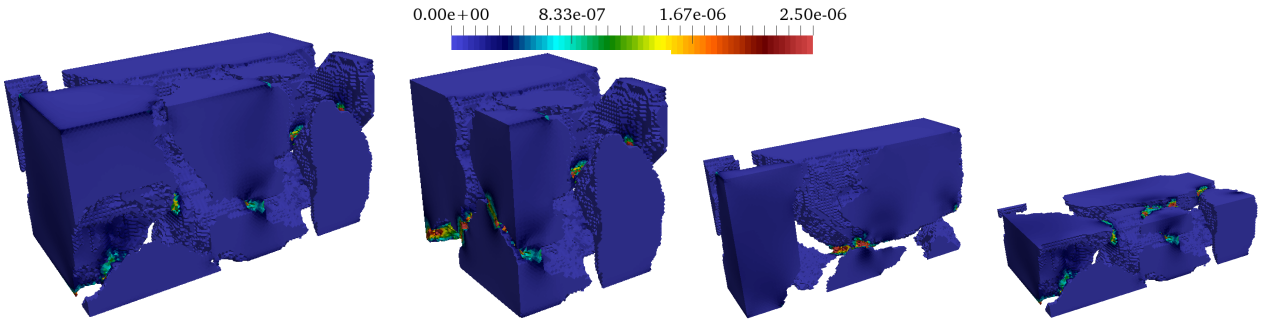

Full view. *xz*-cross section. *yz*-cross section. *xy*-cross section.

Figure 4: Porous rock domain test. The geometry of the true domain Ω, the surrogate domain $\tilde{\Omega}_h$, and contours of the displacement magnitude, the volumetric (pressure) stress and the von Mises stress, for various cross-sections (mid-planes).

References

[1] Grabcad.com: Stent of 1/8" cross section and 1.2" length. https://grabcad.com/library/stent-1-8-across-tube-1-2-length. Accessed: 2016-01-30.

[2] Imperial College Consortium on Pore-scale Modelling: LV60A sandpack. https://figshare.com/articles/LV60A_sandpack/1153795, 10 2014.

[3] Nabil M Atallah, Claudio Canuto, and Guglielmo Scovazzi. The shifted boundary method for solid mechanics. International Journal for Numerical Methods in Engineering, 122(20):5935–5970, 2021.

[4] Mudrak V. Part description and specifications for sponge. https://grabcad.com/library/sponge.